

Communication

## Synthesis and Molecular Structure of *tert*-Butyl 4-(2-*tert*-butoxy-2-oxoethyl)piperazine-1-carboxylate

Constantin Mamat <sup>1,\*</sup>, Anke Flemming <sup>2</sup> and Martin Köckerling <sup>2</sup>

<sup>1</sup> Institut für Radiopharmazie, Helmholtz-Zentrum Dresden-Rossendorf, Bautzner Landstraße 400, D-01328 Dresden, Germany

<sup>2</sup> Institut für Chemie, Anorganische Festkörperchemie, Albert-Einstein-Straße 3a, D-18059 Rostock, Germany; E-Mail: Martin.Koeckerling@uni-rostock.de (M.K.)

\* Author to whom correspondence should be addressed; E-Mail: c.mamat@hzdr.de; Tel.: +49-351-260-2805; Fax: +49-351-260-3232.

Received: 20 December 2011; in revised form: 30 January 2012 / Accepted: 31 January 2012 /

Published: 6 February 2012

---

**Abstract:** The crystal and molecular structure of *tert*-butyl 4-(2-*tert*-butoxy-2-oxoethyl)-piperazine-1-carboxylate is reported. The title compound crystallizes from a petroleum ether/ethyl acetate mixture in the monoclinic space group  $P 2_1/c$  with four molecules in the unit cell. The unit cell parameters are:  $a = 8.4007(2) \text{ \AA}$ ,  $b = 16.4716(4) \text{ \AA}$ ,  $c = 12.4876(3) \text{ \AA}$ ;  $\beta = 90.948(1)^\circ$  and  $V = 1727.71(7) \text{ \AA}^3$ . Bond lengths and angles of this piperazine-carboxylate are typical.

**Keywords:** piperazines; building blocks; X-ray structure

---

### 1. Introduction

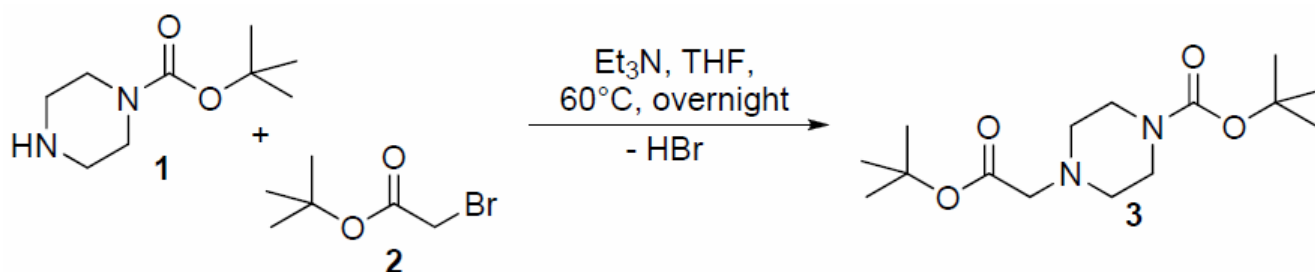
The piperazine moiety plays an important role and is found in various bioactive compounds. In particular, the piperazinoacetic acid motif was found in highly selective factor Xa trypsin-like protease inhibitors [1]. Furthermore, the piperazine residue was used as spacer in pleuromutilin derivatives [2] or as linker in piperazine based hydroxamic acids as histone acylase (HDAC) inhibitors [3]. Functionalized piperazine derivatives were applied in radiopharmaceutical research as starting material for spiro-compounds, which were used for the mild introduction of fluorine-18 [4]. Finally, the acetic acid-piperazine core was used for the linkage of biological active peptides [5]. Alongside to the

convenient reaction of piperazine with haloacetic acid derivatives via nucleophilic substitution, several mild methods were developed using Triton B [6] or  $\text{RuCl}_3$  [7] as catalysts.

## 2. Results and Discussion

The preparation of the title compound *tert*-butyl 4-(2-*tert*-butoxy-2-oxoethyl)piperazine-1-carboxylate (**3**) in a high yield of 79% was accomplished via nucleophilic displacement of the bromine in *tert*-butyl bromoacetate (**2**) with the secondary amine of the Boc-protected piperazine **1** under basic conditions using triethylamine. (Figure 1) The reaction was performed under mild conditions at 60 °C overnight using tetrahydrofuran as solvent. Crystals of **3** were grown during the purification step from a saturated petroleum ether/ethyl acetate solution.

**Figure 1.** The synthesis of title compound **3**.



The crystal and instrumental parameters used in the unit cell determination, the data collection, and structure refinement parameters are summarized in Table 1. The molecular structure of **3** is shown in Figure 2 with the used atom-labeling scheme. The displacement thermal ellipsoids are drawn at the 50% probability level. Selected bond lengths comprising key features of *tert*-butyl 4-(2-*tert*-butoxy-2-oxoethyl)piperazine-1-carboxylate (**3**), are given in Table 2. The central piperazine ring adopts a chair conformation. Whereas the carboxyl unit of the Boc residue, which is attached to N1, is almost in plane with the mean plane of the piperazine ring atoms (22.3°), the plane through the atoms of the second carboxyl unit (C11, O3 and O4) has an angle of 116.3° to the mean plane through the piperazine ring atoms. The packing of the molecules in the unit cell in a view along the crystallographic *a* direction is demonstrated in Figure 3. As visible from this plot, the title molecules have two different but symmetry-related orientations with respect to each other in the crystals of **3**. Intermolecular contacts are limited to those of van-der-Waals type. The shortest intermolecular distances of the polar atoms are between O3 and H atoms of the neighboring molecule at 2.991 Å and between O4 and H atoms at 2.702 and 2.710 Å.

**Figure 2.** A view of the structure of the title molecules in crystals of **3** showing the atom labeling scheme. Displacement ellipsoids are drawn at the 50% probability level.

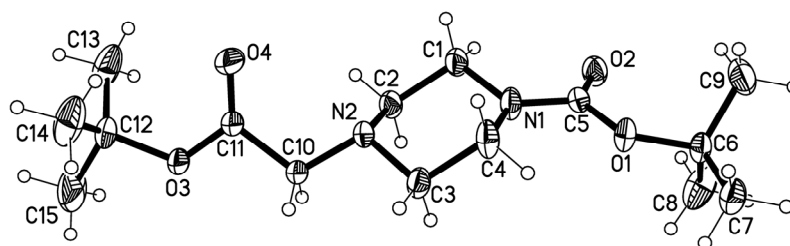


**Table 1.** Crystal data and structure refinement for compound **3**.

Crystal data		Refinement	
Formula	$C_{15}H_{28}N_2O_4$	Refinement method	Full-matrix least-squares on $F^2$
Formula weight	$300.39 \text{ g}\cdot\text{mol}^{-1}$	Data/restraints/parameters	7089/0/190
Temperature	173 K	Measured reflections	52521
Wavelength	$0.71073 \text{ \AA}$	$2 \theta_{\text{max}}$	$68.6^\circ$
Crystal system	monoclinic	$R_{\text{int}}$	2.4%
Space group	$P2_1/c$	Goodness-of-fit on $F^2$	1.04
Unit cell dimensions	$a = 8.4007(2) \text{ \AA}$ $b = 16.4716(4) \text{ \AA}$ $c = 12.4876(3) \text{ \AA}$ $\beta = 90.948(1)^\circ$	Final $R$ indices $[I > 2\sigma(I)]$	$R_1 = 0.0629$ $wR_2 = 0.1791$
Volume	$1727.71(7) \text{ \AA}^3$	$R$ indices (all data)	$R_1 = 0.0801$ $wR_2 = 0.1969$
$Z$	4	Largest diff. peak and hole	$0.97/-0.52 \text{ e}\cdot\text{\AA}^{-3}$
Density (calcd.)	$1155 \text{ g}\cdot\text{cm}^{-3}$		
Absorption coefficient	$0.08 \text{ mm}^{-1}$		
$F(000)$	656		
Crystal size	$0.63 \times 0.42 \times 0.39 \text{ mm}^3$		

**Figure 3.** View of the packing of molecules in crystals of **3** along the crystallographic  $a$  axis.

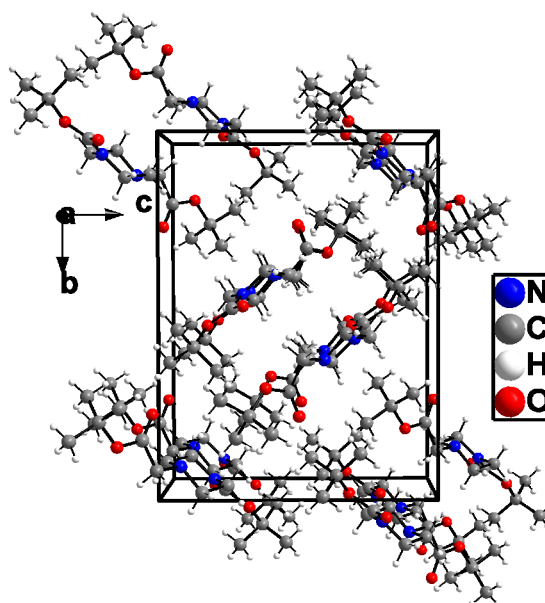


**Table 2.** Selected atom distances [Å] in **3**.

atoms	distance	atoms	distance
N1–C1	1.459(2)	C5–O2	1.220(1)
C1–C2	1.520(2)	O1–C6	1.471(1)
C2–N2	1.463(2)	N2–C10	1.452(1)
N2–C3	1.463(2)	C10–C11	1.516(2)
C3–C4	1.517(2)	C11–O3	1.333(1)
C4–N1	1.466(2)	C11–O4	1.200(2)
N1–C5	1.358(1)	O3–C12	1.477(1)
C5–O1	1.348(1)		

### 3. Experimental Section

#### 3.1. General

NMR spectra were recorded on a Varian Inova-400 and chemical shifts of the  $^1\text{H}$  and  $^{13}\text{C}$  spectra are reported in parts per million (ppm) using tetramethylsilane as internal standard. The melting point was determined on a Galen III (Cambridge Instruments) melting point apparatus (Leica, Vienna, Austria) and is uncorrected. The mass spectrum (MS) was obtained on a Quattro/LC mass spectrometer (MICROMASS) by electrospray ionization.

#### 3.2. Synthesis of *tert*-Butyl 4-(2-*tert*-butoxy-2-oxoethyl)piperazine-1-carboxylate (**3**)

*N*-Boc-piperazine (207 mg, 1.11 mmol) and  $\text{Et}_3\text{N}$  (225 mg, 2.22 mmol) were dissolved in anhydrous THF (10 mL). *tert*-Butyl bromoacetate (434 mg, 2.22 mmol) was added dropwise at ambient temperature and the mixture was stirred at 60 °C overnight. After cooling to room temperature, saturated hydrogen carbonate solution (15 mL) was added and the aqueous layer was extracted with ethyl acetate ( $3 \times 15$  mL). The combined organic layers were dried over  $\text{Na}_2\text{SO}_4$ , the solvent was removed and purification was done via column chromatography (petroleum ether/ethyl acetate = 4:1) to yield **3** as colorless solid (264 mg, 79%). m.p. 102 °C.  $^1\text{H}$  NMR (400 MHz,  $\text{CDCl}_3$ ):  $\delta$  = 1.45 (s, 9H,  $^t\text{Bu}$ ), 1.46 (s, 9H,  $^t\text{Bu}$ ), 2.52 (t,  $^3J = 4.9$  Hz, 4H,  $\text{NCH}_2$ ), 3.12 (s, 2H,  $\text{NCH}_2$ ), 3.47 (t,  $^3J = 4.9$  Hz, 4H,  $\text{NCH}_2$ ).  $^{13}\text{C}$  NMR (101 MHz,  $\text{CDCl}_3$ ):  $\delta$  = 28.3, 28.6 ( $2 \times ^t\text{Bu}$ ), 52.8 ( $\text{NCH}_2$ ), 60.1 ( $\text{NCH}_2$ ), 79.8, 81.4 ( $2 \times \text{C}_{\text{quart}}$ ), 154.8 (C=O). MS (ESI+):  $m/z$  = 323 (11) [ $\text{M}+\text{Na}$ ], 301 (100) [ $\text{M}^++\text{H}$ ].

#### 3.3. Data Collection and Refinement

Crystallographic data were collected with a Bruker-Nonius Apex-X8 CCD-diffractometer with monochromatic  $\text{Mo-K}\alpha$  radiation ( $\lambda = 0.71073$  Å) and a CCD detector. Preliminary data of the unit cell dimensions were obtained from the reflection positions of 36 frames, measured in three different directions of the reciprocal space. After completion of the data measurements the reflection intensities were corrected for Lorentz, polarization, and absorption effects. The data set of 7089 reflections was averaged from 52521 reflections (up to 68.6°) with an internal R value of 2.4% in Laue group 2/m. Averaging in *mmm* (orthorhombic) gives an  $R_{\text{int}}$  larger than 50%, indicating the monoclinic crystal system to be the correct choice. The structures were solved by direct methods using SHELXS-97 and

refined against  $F^2$  on all data by full-matrix least-squares methods using SHELXL-97 version 2 [8,9]. All non-hydrogen atoms were refined anisotropically; all hydrogen atoms bonded to carbon atoms were placed on geometrically calculated positions and refined using riding models. Crystallographic data has been deposited with the Cambridge Crystallographic Data Centre, CCDC-858567. It can be retrieved free of charge through deposit@ccdc.cam.ac.uk or <http://www.ccdc.cam.ac.uk>.

#### 4. Conclusions

The crystal and molecular structure of *tert*-butyl 4-(2-*tert*-butoxy-2-oxoethyl)-piperazine-1-carboxylate (**3**) is reported. These data represent a crystallographically characterized example of a molecular compound with a piperazine building block, which found various applications in the preparation of biological active compounds in pharmaceutical research.

#### References

1. Huang, W.; Naughton, M.A.; Yang, H.; Su, T.; Dam, S.; Wong, P.W.; Arfsten, A.; Edwards, S.; Sinha, U.; Hollenbach, S.; Scarborough, R.M.; Zhu, B.-Y. Design, synthesis, and structure-Activity relationships of unsubstituted piperazinone-Based transition state factor Xa inhibitors. *Bioorg. Med. Chem. Lett.* **2003**, *13*, 723–728.
2. Hirokawa, Y.; Kinoshita, H.; Tanaka, T.; Nakamura, T.; Fujimoto, K.; Kashimoto, S.; Kojima, T.; Kato, S. Pleuromutilin derivatives having a purine ring. Part 2: Influence of the central spacer on the antibacterial activity against Gram-positive pathogens. *Bioorg. Med. Chem. Lett.* **2009**, *19*, 170–174.
3. Rossi, C.; Porcelloni, M.; D'Andrea, P.; Fincham, C.I.; Ettore, A.; Mauro, S.; Squarcia, A.; Bigioni, M.; Parlani, M.; Nardelli, F.; Binaschi, M.; Maggi, C.A.; Fattori, D. Alkyl piperidine and piperazine hydroxamic acids as HDAC inhibitors. *Bioorg. Med. Chem. Lett.* **2011**, *21*, 2305–2308.
4. Grosse-Gehling, P.; Wuest, F.R.; Peppel, T.; Köckerling, M.; Mamat C. 1-(3-[ $^{18}\text{F}$ ]fluoropropyl)piperazines as model compounds for the radiofluorination of pyrido[2,3-*d*]pyrimidines. *Radiochim. Acta* **2011**, *99*, 365–373.
5. Dutta, A.S.; Crowther, M.; Gormley, J.J.; Hassall, L.; Hayward, C.F.; Gellert, P.R.; Kittlety, R.S.; Alcock, P.J.; Jamieson, A.; Moores, J.M.; *et al.* Potent cyclic peptide inhibitors of VLA-4 ( $\alpha_4\beta_1$  integrin)-mediated cell adhesion. Discovery of compounds like cyclo(MePhe-Leu-Asp-Val-D-Arg-D-Arg) (ZD7349) compatible with depot formulation. *J. Peptide Sci.* **2000**, *6*, 321–341.
6. Meshram, H.M.; Chennakesava Reddy, B.; Ramesh Goud, P. Triton B-Mediated Mild, Convenient, and Efficient Method for the Selective Alkylation of Cyclic Secondary Amines and Thiols. *Synth. Commun.* **2009**, *39*, 2297–2303.
7. Varala, R.; Enugala, R.; Adapa, S.R. Ruthenium(III) chloride-catalyzed efficient protocol for ethyl diazoacetate insertion into the N–H bond of secondary amines. *Monatsh. Chem.* **2008**, *139*, 1369–1372.
8. Sheldrick, G.M. *SHELXS/L-97, Programs for the Solution and Refinement of Crystal Structures*; University of Göttingen: Göttingen, Germany, 1997.

9. Sheldrick, G.M. A short history of *SHELX*. *Acta Cryst.* **2008**, *A64*, 112–122.

© 2012 by the authors; licensee MDPI, Basel, Switzerland. This article is an open access article distributed under the terms and conditions of the Creative Commons Attribution license (<http://creativecommons.org/licenses/by/3.0/>).